iScience

Article

Contribution of intact viral genomes persisting in blood and tissues during ART to plasma viral rebound in SHIV-infected rhesus macaques

Graphical abstract

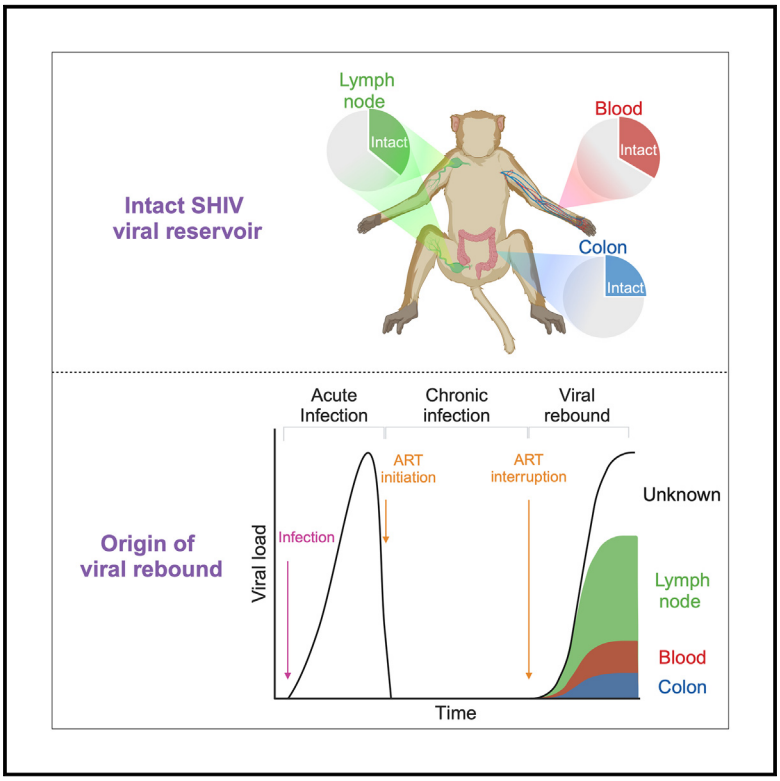

Authors

César Trifone, Corentin Richard, Amélie Pagliuzza, ..., Andrés Finzi, David T. Evans, Nicolas Chomont

Correspondence

nicolas.chomont@umontreal.ca

In brief

Genomics; Virology

Highlights

- Clonal expansions of SHIV-infected cells are rare in macaques receiving ART
- There was no evidence of viral compartmentalization between blood and tissues
- Lymph nodes harbor a larger proportion of intact SHIV genomes compared to the colon
- Rebounding viruses frequently matched intact proviruses retrieved from lymph nodes

Trifone et al., 2025, iScience *28*, 111998
March 21, 2025
https://doi.org/10.1016/j.isci.2025.111998

CellPress

iScience

CellPress
OPEN ACCESS

Article

Contribution of intact viral genomes persisting in blood and tissues during ART to plasma viral rebound in SHIV-infected rhesus macaques

César Trifone,[1,2] Corentin Richard,[3] Amélie Pagliuzza,[1] Caroline Dufour,[1] Audrée Lemieux,[1] Natasha M. Clark,[4] Sanath K. Janaka,[4] Christine M. Fennessey,[5] Brandon E. Keele,[5] Rémi Fromentin,[1,2] Jacob D. Estes,[6,7] Daniel E. Kaufmann,[1,2,8,9] Andrés Finzi,[1,2] David T. Evans,[4] and Nicolas Chomont[1,2,10,*]

[1]Centre de Recherche du CHUM, Montréal, QC H2X 0A9, Canada
[2]Département de Microbiologie, infectiologie et immunologie, Faculté de Médecine, Université de Montréal, Montréal, QC H3T 1J4, Canada
[3]University College of London, London, England WC1E 6BT, UK
[4]Wisconsin National Primate Research Center, University of Wisconsin-Madison, Madison, WI 53707, USA
[5]AIDS and Cancer Virus Program, Frederick National Laboratory for Cancer Research, Frederick, MD 21701, USA
[6]Vaccine and Gene Therapy Institute, Oregon Health & Science University, Beaverton, OR 97239, USA
[7]Oregon National Primate Research Center, Oregon Health & Science University, Beaverton, OR 97239, USA
[8]Département de Médecine, Université de Montréal, Montréal, QC H3T 1J4, Canada
[9]Division of Infectious Diseases, Department of Medicine, Lausanne University Hospital and University of Lausanne, 1011 Lausanne, Switzerland
[10]Lead contact
*Correspondence: nicolas.chomont@umontreal.ca
https://doi.org/10.1016/j.isci.2025.111998

SUMMARY

Persistent SIV/HIV reservoirs are the primary obstacle to a cure and the source of viral rebound after ART interruption (ATI). However, the anatomical source of viral rebound remains elusive. Here, we characterized the proviral landscape in the blood, inguinal, and axillary lymph nodes and colon biopsies of five SHIV-infected rhesus macaques (RMs), under ART for 28 weeks. From the 144 near full-length (NFL) proviral sequences obtained pre-ATI, 35% were genetically intact and only 2.8% were found in multiple copies. Envelope sequences of plasma rebounding viruses after ATI, more frequently matched pre-ATI intact proviruses retrieved from lymph nodes compared to sequences isolated from the blood or the colon (4, 1, and 1 pair of matched sequences, respectively). Our results suggest that clonal expansion of infected cells rare in this model, and that intact proviruses persisting in the lymph nodes may be a preferential source of viral rebound upon ATI.

INTRODUCTION

HIV reservoirs represent the predominant barrier to a cure for HIV infection. Latently infected cells persist despite antiretroviral therapy (ART) and are the source of viral rebound upon analytical treatment interruption (ATI).[1–5] Most of the proviruses persisting during ART have genetic defects that impede their ability to replicate,[6–8] although they may retain a capacity to produce short viral transcripts or proteins.[9–13] Only a small proportion of the viral reservoir is made of genetically intact proviruses that have the potential to produce viral progeny[1,3,7] and distinguishing those from the rest of the viral reservoir requires sophisticated approaches.[14–17] A second obstacle stems from the location of HIV-infected cells, which are primarily found in anatomic compartments throughout the organism.[18–23] For these reasons, characterizing viral reservoirs in deep tissues is a challenge in people with HIV (PWH) but is more manageable in non-human primate models (NHP) of SIV/SHIVinfection.[18,23,24]

It is well-established that SIV can disseminate in several compartments including the spleen, lymph nodes, gut, brain, blood, liver, and lungs by infecting not only CD4 T cells but also resident macrophages.[25–28] Additionally, many of these tissues have been identified as preferential sites for viral persistence and potential sources of viral resurgence following ART interruption.[29,30] These newly produced viral particles emerge from replication competent reservoirs,[15] but despite many attempts to identify the source of this viral rebound,[29,31,32] the precise origin of these virions remains elusive.

Several NHP models have been developed to study the mechanisms responsible for the persistence of HIV in humans. These animal models largely reproduce the observations made in humans, with viral RNA being detected in the plasma within days or weeks following ART cessation.[33,34] Similar to HIV, the majority of SIV genomes persisting during ART have genetic defects, particularly large deletions. However, several studies reported higher proportions of intact proviruses in the SIV reservoir (30–60%) compared to the HIV reservoir (5–10%).[11,22,35,36] This difference may be attributed to a greater ability of SIV and SHIV to establish a larger intact reservoir compared to HIV, to the prompter initiation of ART in animal models which limits the

accumulation of defective proviruses compared to natural infection in humans or to the shorter duration of ART.[35,36] Like in HIV, genetically intact SIV genomes decay faster than defective proviruses but the kinetic may depend on the viruses, with SIV displaying a three phasic decay whereas SHIV better fits a two-phase decay model.[37,38] Importantly, unlike in PWH on ART for many years, both the SIV and SHIV reservoirs are composed of a relatively large proportion of unintegrated genomes which could complicate the analysis. Excluding these unintegrated forms may be a prerequisite to draw meaningful conclusions on the dynamic of the long-lived viral reservoir, which is mainly composed of integrated viral genomes.[36–38]

Here, we analyzed the proviral populations in three compartments (blood, lymph nodes, and colon) from SHIV-infected rhesus macaques (RMs) on ART. Using an optimized near full-length sequencing approach, we studied the genetic integrity and clonality of the proviral landscape in each compartment. In an attempt to identify the source of viral resurgence, we compared the proviral sequences obtained before ATI with those from the plasma rebounding viruses.

RESULTS

Cohort characteristics and reservoir quantification

Five RMs of Indian ancestry were inoculated intravenously with SHIV-AD8-EO (Figure 1A). After 8 weeks, the animals initiated a combination ART regimen of tenofovir, emtricitabine and dolutegravir and maintained on ART for 28 weeks. Cohort characteristics are described in Table S1 (Table S1). All animals achieved viral suppression after 24 weeks of ART (week 32 post infection), although small blips (< 65 SHIV RNA copies per mL) were detected in 2 animals (Figure 1B). Following ART interruption, at week 37 pi, viral rebound was observed in all animals within 1–2 weeks.

We first measured SHIV DNA in blood, peripheral lymph node and colon from all 5 animals at 2 time points before ATI (weeks 34 and 36) and at 2 time points following ATI (weeks 38 and 40). Minimal changes were noted in the frequencies of cells harboring SHIV DNA in blood and lymph nodes over time, whereas frequencies of infected cells were lower and more variable in the colon (Figure 1C). Measured frequencies of infected cells were lower in the colon compared to blood and lymph node at all time points (Figure S1A). Cell-associated SHIV RNA levels were low or undetectable in all compartments during ART, and, as expected, increased significantly in all samples following ATI (Figure 1D). Of note, this increase in the transcriptional activity of the reservoir during ATI was more pronounced in the blood compared to the lymph node and the colon (Figure S1).

SHIV viral reservoir showed low levels of clonality and a relevant proportion of intact proviruses

To analyze the proviral landscape in blood and tissues from virally suppressed SHIV infected animals, we applied a novel approach to amplify and sequence near full-length SHIV genomes from blood, colon, and lymph nodes collected before ATI (weeks 34 and 36). We obtained a total of 144 sequences from the 5 animals from week 34 and 36 (pre-ATI time points) (from 32 to 41 for each animal: 49 from the blood, 63 from the lymph nodes, and 32 from the colon) (Figure 2). 2-LTR circles, which yielded a PCR product of ~700 bp (see STAR Methods), represented 80.6%, 67.8%, and 76.7% of all amplicons retrieved from blood, lymph nodes, and colon, respectively (Figure S2), and were excluded from the analysis.

We built phylogenetic trees of sequences derived from each individual animal to analyze the SHIV proviral population in each tissue (Figure 3). In all 5 animals, proviruses derived from different anatomical sites appeared intermingled in the phylogenetic tree, suggesting the absence of viral compartmentalization in this model. We then assessed viral diversity in each compartment using the founder strain SHIV-AD8-EO as a reference. There was a trend for a higher degree of viral diversity in the colon compared to blood and lymph node, but this difference did not reach statistical significance (Figure S3).

We then analyzed the genetic integrity of the proviruses retrieved from all animals in blood, lymph node and colon using the pipeline described in Figure 2. Large deletions represented the main type of defect in all compartments (Figure 4A), with other types of defects being relatively rare. Overall, 35.6% of all proviral sequences were genetically intact. Colon biopsies contained a lower proportion of intact genomes (25.0%) compared to lymph node (46.7%) and blood (37.5%) ($p < 0.05$, Figure 4A).

We then measured the clonality of the SHIV reservoir in these compartments. Identical sequences represented only 2.8% of all sequences analyzed (2 identical sequences in the blood of one animal and 2 identical sequences in the colon of another animal), suggesting that clonal expansion of SHIV-infected cells was limited in these animals who had been on ART for a relatively short period of time (Figure 4B).

Rebounding viruses were more genetically related to intact proviruses residing in the lymph node

To identify the anatomical source of viral rebound after ART discontinuation, we compared sequences derived from rebounding plasma virions to those from the viral reservoir before ATI. 95 sequences of the *env* gene from plasma virions were obtained from all 5 animals (between 14 and 24 for each animal). In 3 out of 5 animals, the *env* sequences from these virions were identical to genetically intact proviral genomes sampled pre-ATI. In animal 09082, 2 virion-derived sequences matched an intact proviral sequence recovered from lymph nodes (Figure 5A). This was also observed in animal 10075, in whom a plasma virion-derived sequence matched a pre-ATI genetically intact sequence from lymph node. In this same animal, 5 plasma virion-derived sequences were identical to intact proviruses sequences retrieved from lymph node ($n = 3$) and colon ($n = 1$) (Figure 5A middle row). In animal 14090, a virion-derived sequence matched genetically intact sequences isolated from lymph nodes ($n = 3$) and blood ($n = 3$) collected pre-ATI (Figure 5A last row).

We then calculated the median genetic distance between virion-derived sequences and sequences of genetically intact proviruses sampled from each tissue pre-ATI. In all animals, the minimal genetic distance was found between plasma virions sequences and proviral sequences isolated from lymph nodes rather than those retrieved from the blood or the colon (Figure 5B). Overall, virion-derived env sequences were genetically

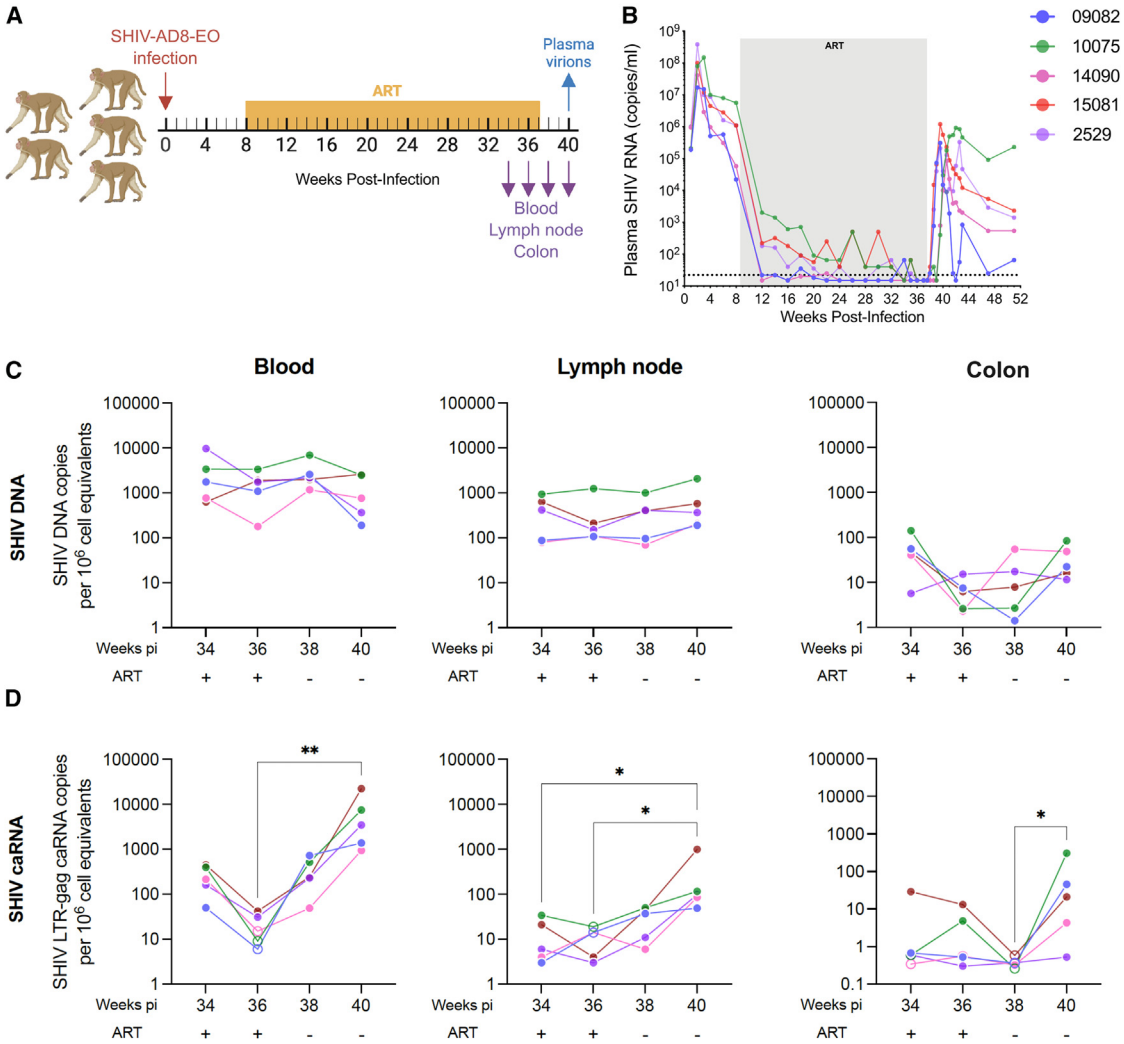

Figure 1. Study design and quantification of reservoir markers

(A) Schematic representation of the study and sampling schedule. Five rhesus macaques were infected intravenously with SHIV-AD8-EO (red arrow) and treated with ART from week 8 to week 37 (orange box). Violet arrows indicate blood, lymph nodes, and colon-sampling time points. Plasma virions *env* sequences were obtained from blood at week 40 (blue arrow).

(B) Longitudinal plasma viral load measures in the 5 animals. The gray area indicates time on ART.

(C) Quantification of SHIV DNA. Results are shown for blood, lymph nodes, and colon and represented as SHIV DNA copies per million CD4 T cells (blood and lymph node) or per million total cells (colon).

(D) Quantification of SHIV cell-associated RNA (LTR-gag). Results are shown for blood, lymph node, and colon and represented as SHIV RNA copies per million CD4 T cells (blood and lymph node) or per million total cells (colon). Undetectable measurements are represented by open symbols, and limits of detection are plotted. Statistical analysis was performed by a parametric one-way ANOVA test and Dunn's multiple comparison post-test. *$p < 0.05$; **$p < 0.01$.

closer to pre-ATI intact proviral sequences retrieved from lymph node than from blood or the colon (Figure 5C). Taken together, these results indicate that plasma rebound viruses are genetically closer to proviruses derived from lymph nodes compared to blood and colon, suggesting that the lymphoid tissue may be a preferential source or viral rebound in this model.

DISCUSSION

In this study, we analyzed the blood and tissue viral reservoirs in 5 SHIV-infected RMs receiving ART. We combined ultrasensitive measures of SHIV DNA/RNA and near full-length genome sequencing to analyze the dynamics of reservoir markers in longitudinal samples collected before and after ATI. SHIV DNA copy numbers remained relatively stable in blood and lymph nodes during ART and after ATI, indicating that the size of the pool of infected cells does not dramatically increase in the first weeks of viral rebound. In contrast, the transcriptional activity of the viral reservoir, which was below the limit of detection of our assay in the majority of these tissues during ART, rapidly increased in all compartments upon ATI. Both DNA and RNA measures in colon biopsies were highly variable between

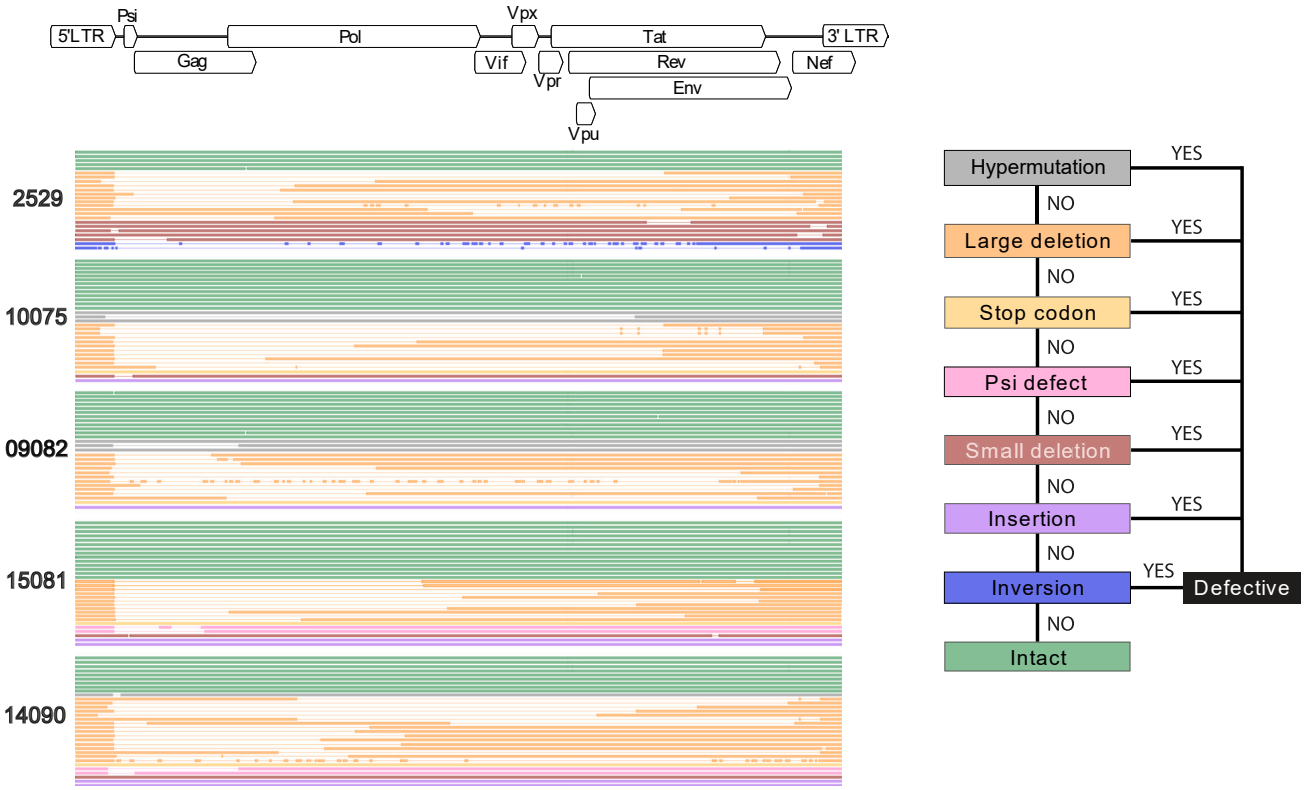

Figure 2. SHIV proviral landscape in the 5 animals

The SHIV-AD8-EO genome diagram at the top illustrates the coverage of the near-full length (NFL) amplification (92%). Each horizontal line represents and individual proviral sequence obtained by NFL amplification from week 34 and 36 (pre-ATI time points). Each block of sequences derived from a given animal is identified with the corresponding animal ID. The type of defect in each sequence is indicated by a specific color, as shown in the diagram on the right. Alignments were performed using the founder strain SHIV-AD8-EO as a reference.

animals and between time points, which likely reflected the heterogeneity of the gut tissue and the challenge of conducting quantitative analysis using small biopsies from this large organ.

Using an optimized approach to obtain near full-length SHIV genome sequences, we amplified 144 NFL proviral genomes and built phylogenetic trees to study the viral diversity in each compartment during ART. Sequences derived from the blood, lymph nodes, and colon appeared intermingled, suggesting a lack of compartmentalization of viral sequences between the three sites. Proviral sequences retrieved from the colon were genetically more distant from the founder viral strain (SHIV-AD8-EO) compared to those isolated from the lymph node and the blood, suggesting that enhanced levels of SHIV replication may have resulted in heightened diversity in this site.

More than a third of all proviral sequences were genetically intact, which likely results from the fact that ART was initiated relatively early after infection, as reported before.[35,36] The prompt initiation of ART may have limited the accumulation of mutations in archived proviral sequences, whereas the short period on ART might also mask the decay of the intact reservoir through time. Consistent with previous reports,[35,36] large deletions represented the main defect identified in the SHIV reservoir. The proportion of intact genomes was significantly higher in the lymph node (46%) and the blood (37%) compared to the colon (25%), suggesting that lymph nodes may represent a preferential site for the persistence of genetically intact proviruses, in line with previous studies.[35,36,39] The lower percentage of intact proviruses in the colon is coincident with increased proportions of hypermutated genomes and proviruses with premature stop codons. This may be attributed to the abundance of activated $CD4^+$ T cells in the colon, which are characterized by heightened expression of APOBEC3G compared to resting $CD4^+$ T cells.[40]

It is well-established that the proliferation of latently infected cells is a major mechanism of HIV persistence during ART.[41–46] In our cohort of animals, the SHIV reservoir was constituted of an overwhelming majority of unique proviral sequences in all 3 compartments, as previously observed in the blood of SHIV-infected animals[36] as well as in the blood and lymph nodes of SIV-infected animals.[32] Our results confirm and extend these results by showing that clonal expansion of SHIV-infected cells is also rare in tissues, which was expected in these animals who had been on ART for only 29 weeks. Of note, a study in which integration site sequencing was used as a measure of clonality reported that clonal expansions can occur in SIV-infected macaques on suppressive ART after only one year.[47] In this study, the size of the expanded clones was small, suggesting that we may have missed small clonal expansions in our study because of the relatively limited number of proviruses we obtained.

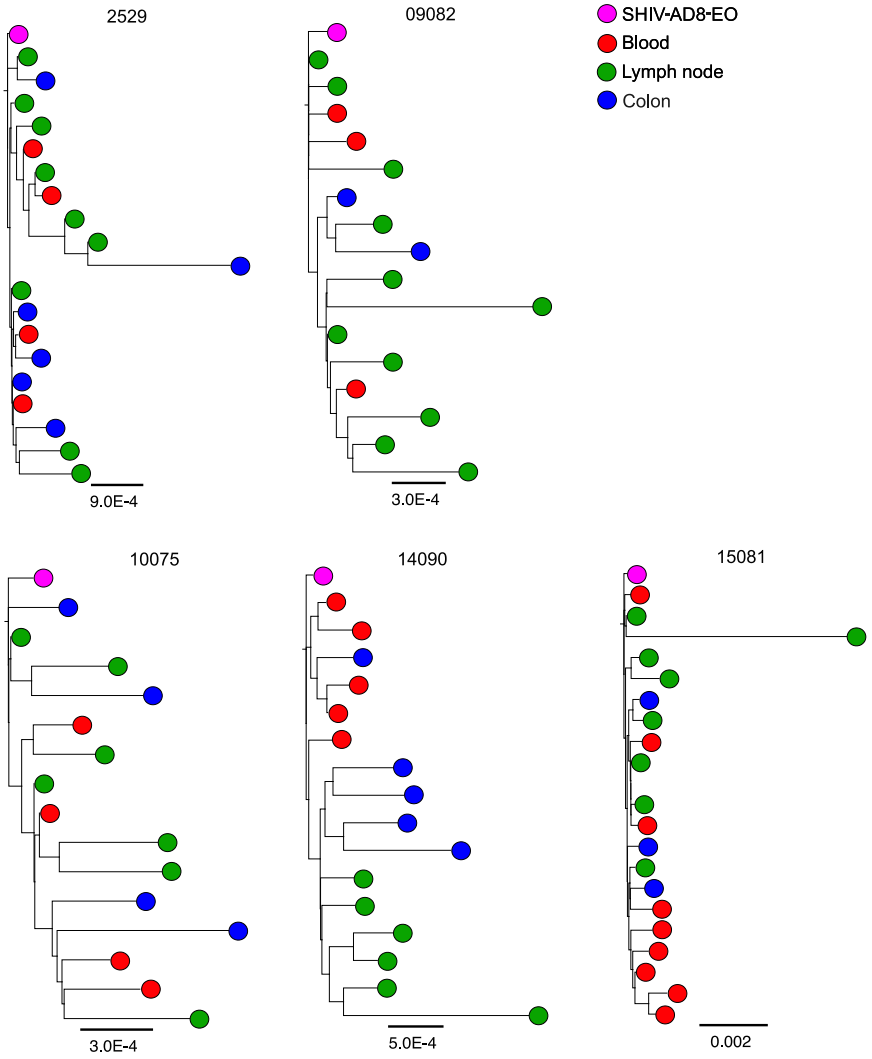

Figure 3. Phylogenetic trees SHIV NFL sequences

Phylogenetic trees were built with all sequences obtained from each animal, after excluding the proviral sequences identified as hypermutated. Trees were built using the estimated by maximum likelihood model rooted to the reference sequence of the founder strain SHIV-AD8-EO (pink). Sequences derived from the different compartments are identified by a specific color: red for the blood, green for the lymph node, and blue for the colon. Scale bars refer to the phylogenetic distance, represented by the length of the branch, in nucleotide substitution per site.

We then compared proviral sequences retrieved from samples collected during ART with env sequences derived from rebounding plasma virion during ATI. We chose the env gene because of its genetic diversity, in both SIV and HIV infections.[29,36] Since our goal was to identify tissues that may represent a source of viral rebound, we focused our analysis on genetically intact proviral sequences. We identified 4 pairs of matched sequences between intact proviruses in the lymph node and virion-derived sequences. Of note, two of these 4 sequences were not shared with any other compartment, whereas the other two were shared between the lymph node and the blood or the colon. This was in line with the fact that virion-derived sequences were genetically closer to lymph node proviral sequences than genomes amplified from the blood or the colon. Altogether, these observations may suggest that rebounding viruses may be preferentially produced by genetically intact proviruses that persisted in lymph nodes during ART.

Several studies reported that ATI is characterized by a rapid viral reactivation in several tissues throughout the body,[4,29] suggesting a multifocal recrudescence of viral replication after ART interruption, both in humans and in non-human models of HIV infection.[4,29] Consistent with our observations in SHIV-infected RMs, proviruses residing in the lymphoid tissue have been suggested as a preferential source of SIV rebound.[30,32] Both the SIV and SHIV experimental models are therefore consistent with the observations made in PWH undergoing ATI in whom viral resurgence is thought to originate from the lymphoid tissue.[4] Several intrinsic characteristics of lymph nodes likely contribute to their capacity to serve as preferential sites of viral persistence and resurgence: (1) lymph nodes are enriched in T follicular helper (Tfh) cells, which are known to be highly susceptible to HIV/SIV infection[48]; (2) they are characterized by the presence of well-structured B follicles in which infected Tfh cells reside and from which cytotoxic CD8 T cells are largely excluded[49,50]; (3) follicles also contain follicular dendritic cells which can retain infectious viral particles on their surface for years,[39,51] (4) lymph nodes contain a high-density of CD4 T cells, the primary target cell of HIV, SIV and SHIV-AD8. Altogether, these characteristics and our observations suggest that lymphoid tissues are important contributors to the persistence of the rebound competent HIV reservoir. Therapeutic strategies aimed at eliminating the viral reservoir or controlling viral rebound should be optimized to penetrate these complex structures.

Limitations of the study

This study presents several limitations. We studied samples from 5 animals which had been infected for a short period of time before starting an ART regime, which could have an impact on viral evolution and clonality of the viral reservoir. Additionally, the time on ART was relatively short (29 weeks) when treatment was interrupted. Given that full suppression on ART may require longer treatment, we cannot exclude the possibility that ongoing viral replication still occurred in these animals at the time of ATI.

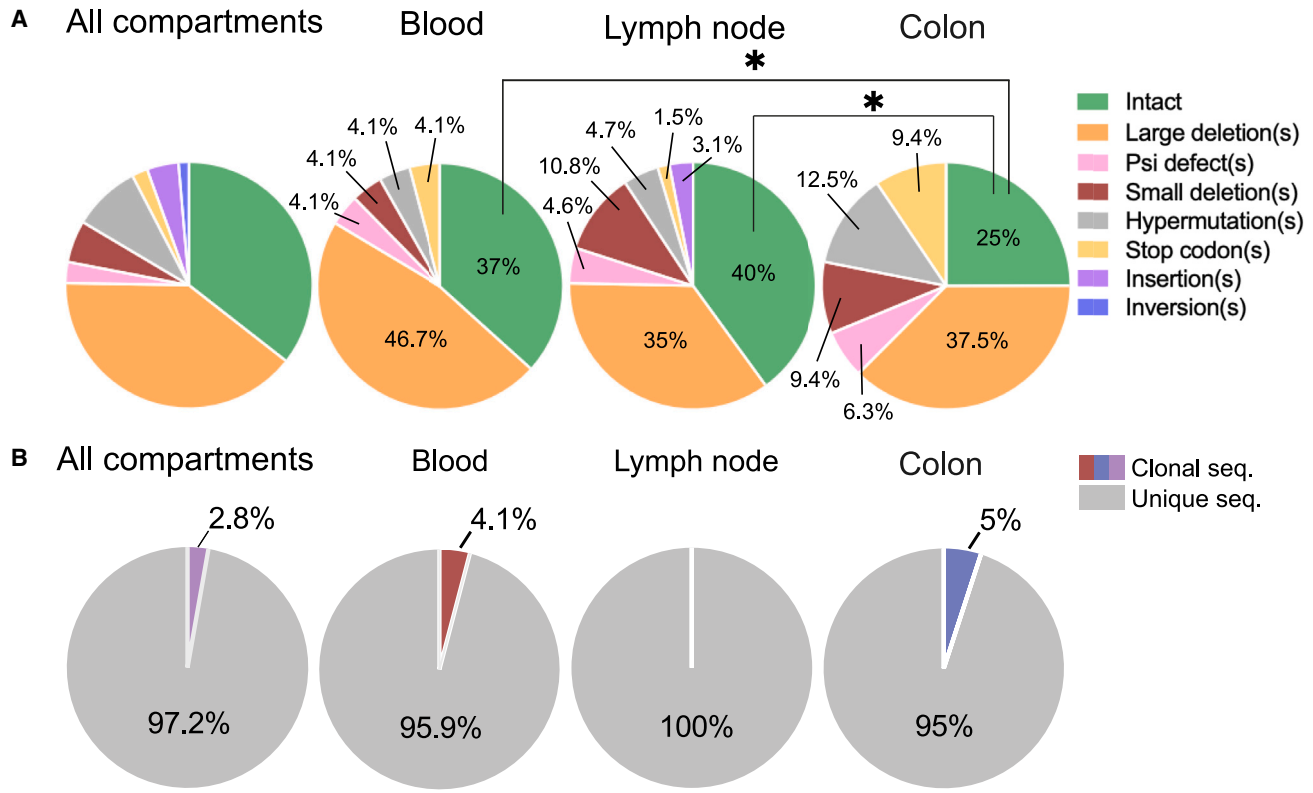

Figure 4. Genetic intactness and clonality of SHIV genomes

(A) Pie chart summarizing the proportion of genomes retrieved from each compartment displaying a specific type of genetic defect.

(B) Pie chart representing the proportion of identical proviral sequences in each compartment. Clones are identified by a different color. Unique sequences are shown in gray. Statistical analysis was performed by a two-way ANOVA test and Tukey's multiple comparison post-test. *$p < 0.05$.

The relatively small number of NFL sequences may have limited our ability to detect clonal expansions in the reservoir. In addition, since we obtained a larger number of proviruses from lymph nodes ($n = 63$) compared to blood ($n = 49$) and colon biopsies ($n = 32$), we cannot exclude the possibility that under sampling in these two compartments may have limited our ability to detect proviruses contributing to viral rebound.

We sequenced the whole SHIV envelope to perform the analysis regarding the origin of the viral rebound, which is the most variable region of the viral genome and provides a representative picture of the viral diversity. However, we cannot exclude the existence of genetic variation outside the *env* gen region that could mask ours results.

Due to the limited sample size in this study (2 females and 3 males), we cannot draw definitive conclusions regarding the impact of sex on the evidence presented.

RESOURCE AVAILABILITY

Lead contact

Requests for further information and resources should be directed to and will be fulfilled by the lead contact, Nicolas Chomont (nicolas.chomont@umontreal.ca).

Materials availability

This study did not generate new unique reagents.

Data and code availability

- Data: Sequences are available on-line with the ID number: GenBank: BankIt2875156 (PQ380606-PQ380700), GenBank: BankIt2921480 (PV068831 - PV068975).
- Code: pbAA PacBio algorithm v1.0.3 https://github.com/PacificBiosciences/pbAA
- Any additional information required to reanalyze the data reported in this paper is available from the lead contact upon request.

ACKNOWLEDGMENTS

We thank the flow cytometry core at the CRCHUM, managed by Gael Dulude and Philippe St-Onge for cell sorting. We thank Dr. Malcom Martin (NIAID) for kindly providing with the challenge virus SHIV-AD8-EO used in this project. The following reagents were obtained through the NIH HIV Reagent Program, Division of AIDS, NIAID, NIH: Simian Immunodeficiency Virus, mac316 infected CEMx174 Cells, Clone 3D8. This work was partially supported by National Institute of Allergy and Infectious Disease of the National Institutes of Health under award numbers 5R01AI149672 and UM1AI164560 (Delaney AIDS Research Enterprise, DARE), the Canadian Institutes for Health Research (CIHR; operating grant PJT175106 and the Canadian HIV Cure Enterprise (CanCURE) team grant HB2 - 164064), the Réseau SIDA et maladies infectieuses du Fonds de Recherche du Québec - Santé (FRQ-S). This project has also been funded in part by the National Institutes of Health grant P51 OD011092 awarded to the Oregon National Primate Research Center (J.D.E.) and with federal funds from the National Cancer Institute, National Institutes of Health, under contract no. 75N91019D00024/HHSN261201500003I. The content of this publication does not necessarily reflect the views or policies

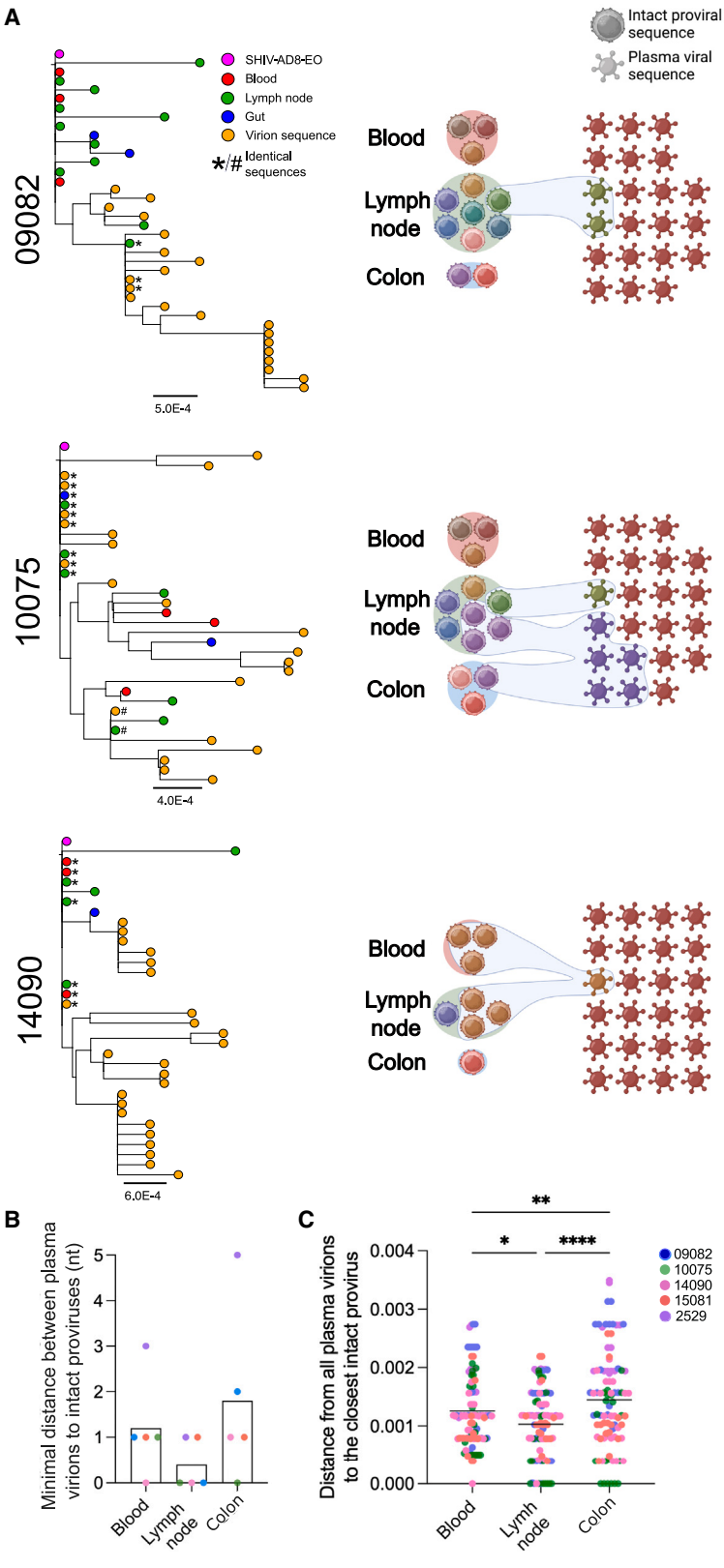

Figure 5. Phylogenetic relationships between genetically intact sequences isolated from pre-ATI samples and rebounding viruses

(A) Left column: phylogenetic trees of genetically intact proviral sequences from pre-ATI samples and sequences of rebounding viruses. Proviral sequences matching rebound virion sequences are indicated by a hash or an asterisk. Right column: diagram representing the fraction of rebounding viruses that are genetically identical to an intact provirus retrieved from a pre-ATI sample.

(B) Minimal genetic distance between the sequence of a rebounding plasma virions and a genetically intact provirus was calculated for all compartments and in all animals.

(C) Genetic distances between each rebounding plasma virions and the closest intact proviral sequence from each compartment for all compartments and in all animals. Statistical analysis was performed by a one-way ANOVA test and Tukey's multiple comparison post-test. $^{**}p < 0.01$; $^{***}p < 0.001$.

of the Department of Health and Human Services, nor does mention of trade names, commercial products, or organizations imply endorsement by the U.S. Government. Furthermore, the funders had no role in study design, data collection and analysis, decision to publish, or preparation of the manuscript.

AUTHOR CONTRIBUTIONS

C.T. designed and performed the experiments, analyzed the data, and wrote the manuscript. C.R. performed the bioinformatics analyses of the sequencing data. N.M.C. and S.K.J. designed and performed part of the experiments. A.P., C.M.F., and B.E.K. performed part of the experiments. A.L. performed the informatic processing of the data and provided conceptual advice. C.D., J.D.E., and D.E.K. provided conceptual advice and manuscript edits. R.F. provided conceptual advice, analyzed the data and reviewed the manuscript. D.T.E. designed the experiments and provided conceptual advice. A.F. designed the experiments. N.C. designed the experiments, analyzed the data, and wrote the manuscript. All authors read, edited, and approved the manuscript.

DECLARATION OF INTERESTS

The authors declare no competing interests.

STAR★METHODS

Detailed methods are provided in the online version of this paper and include the following:

- KEY RESOURCES TABLE
- EXPERIMENTAL MODEL AND STUDY PARTICIPANT DETAILS
- METHOD DETAILS
  - DNA and RNA extractions
  - SHIV DNA and RNA quantifications
  - Near full-length amplification of SHIV genomes
  - PacBio sequencing
  - PacBio demultiplexing and cleaning
  - Integrity analysis
  - Clonality analysis
  - Env sequencing
- QUANTIFICATION AND STATISTICAL ANALYSIS

SUPPLEMENTAL INFORMATION

Supplemental information can be found online at https://doi.org/10.1016/j.isci.2025.111998.

Received: November 26, 2024
Revised: November 26, 2024
Accepted: February 7, 2025
Published: February 11, 2025

REFERENCES

1. Finzi, D., Hermankova, M., Pierson, T., Carruth, L.M., Buck, C., Chaisson, R.E., Quinn, T.C., Chadwick, K., Margolick, J., Brookmeyer, R., et al. (1997). Identification of a Reservoir for HIV-1 in Patients on Highly Active Antiretroviral Therapy. Science *278*, 1295–1300. https://doi.org/10.1126/science.278.5341.1295.
2. Chun, T.-W., Stuyver, L., Mizell, S.B., Ehler, L.A., Mican, J.A., Baseler, M., Lloyd, A.L., Nowak, M.A., and Fauci, A.S. (1997). Presence of an inducible HIV-1 latent reservoir during highly active antiretroviral therapy. Proc. Natl. Acad. Sci. USA *94*, 13193–13197. https://doi.org/10.1073/pnas.94.24.13193.
3. Wong, J.K., Hezareh, M., Gunthard, H.F., Havlir, D.V., Ignacio, C.C., Spina, C.A., and Richman, D.D. (1997). Recovery of Replication-Competent HIV Despite Prolonged Suppression of Plasma Viremia. Science *278*, 1291–1295. https://doi.org/10.1126/science.278.5341.1291.
4. Rothenberger, M.K., Keele, B.F., Wietgrefe, S.W., Fletcher, C.V., Beilman, G.J., Chipman, J.G., Khoruts, A., Estes, J.D., Anderson, J., Callisto, S.P., et al. (2015). Large number of rebounding/founder HIV variants emerge from multifocal infection in lymphatic tissues after treatment interruption. Proc. Natl. Acad. Sci. USA *112*, E1126–E1134. https://doi.org/10.1073/pnas.1414926112.
5. Li, J.Z., Melberg, M., Kittilson, A., Abdel-Mohsen, M., Li, Y., Aga, E., Bosch, R.J., Wonderlich, E.R., Kinslow, J., Giron, L.B., et al. (2024). Predictors of HIV rebound differ by timing of antiretroviral therapy initiation. JCI Insight *9*, e173864. https://doi.org/10.1172/jci.insight.173864.
6. Bruner, K.M., Murray, A.J., Pollack, R.A., Soliman, M.G., Laskey, S.B., Capoferri, A.A., Lai, J., Strain, M.C., Lada, S.M., Hoh, R., et al. (2016). Defective proviruses rapidly accumulate during acute HIV-1 infection. Nat. Med. *22*, 1043–1049. https://doi.org/10.1038/nm.4156.
7. Pasternak, A.O., and Berkhout, B. (2016). HIV Reservoir: Finding the Right Needles in a Needlestack. Cell Host Microbe *20*, 280–282. https://doi.org/10.1016/j.chom.2016.08.011.
8. Bruner, K.M., Wang, Z., Simonetti, F.R., Bender, A.M., Kwon, K.J., Sengupta, S., Fray, E.J., Beg, S.A., Antar, A.A.R., Jenike, K.M., et al. (2019). A quantitative approach for measuring the reservoir of latent HIV-1 proviruses. Nature *566*, 120–125. https://doi.org/10.1038/s41586-019-0898-8.
9. Pollack, R.A., Jones, R.B., Pertea, M., Bruner, K.M., Martin, A.R., Thomas, A.S., Capoferri, A.A., Beg, S.A., Huang, S.-H., Karandish, S., et al. (2017). Defective HIV-1 Proviruses Are Expressed and Can Be Recognized by Cytotoxic T Lymphocytes, which Shape the Proviral Landscape. Cell Host Microbe *21*, 494–506. https://doi.org/10.1016/j.chom.2017.03.008.
10. Takata, H., Mitchell, J.L., Pacheco, J., Pagliuzza, A., Pinyakorn, S., Buranapraditkun, S., Sacdalan, C., Leyre, L., Nathanson, S., Kakazu, J.C., et al. (2023). An active HIV reservoir during ART is associated with maintenance of HIV-specific CD8+ T cell magnitude and short-lived differentiation status. Cell Host Microbe *31*, 1494–1506. https://doi.org/10.1016/j.chom.2023.08.012.
11. Dufour, C., Richard, C., Pardons, M., Massanella, M., Ackaoui, A., Murrell, B., Routy, B., Thomas, R., Routy, J.-P., Fromentin, R., and Chomont, N. (2023). Phenotypic characterization of single CD4+ T cells harboring genetically intact and inducible HIV genomes. Nat. Commun. *14*, 1115. https://doi.org/10.1038/s41467-023-36772-x.
12. Sannier, G., Dubé, M., Dufour, C., Richard, C., Brassard, N., Delgado, G.G., Pagliuzza, A., Baxter, A.E., Niessl, J., Brunet-Ratnasingham, E., et al. (2021). Combined single-cell transcriptional, translational, and genomic profiling reveals HIV-1 reservoir diversity. Cell Rep. *36*, 109643. https://doi.org/10.1016/j.celrep.2021.109643.
13. Dubé, M., Tastet, O., Dufour, C., Sannier, G., Brassard, N., Delgado, G.-G., Pagliuzza, A., Richard, C., Nayrac, M., Routy, J.-P., et al. (2023). Spontaneous HIV expression during suppressive ART is associated with the magnitude and function of HIV-specific CD4+ and CD8+ T cells. Cell Host Microbe *31*, 1507–1522. https://doi.org/10.1016/j.chom.2023.08.006.
14. Wang, Z., Simonetti, F.R., Siliciano, R.F., and Laird, G.M. (2018). Measuring replication competent HIV-1: advances and challenges in defining the latent reservoir. Retrovirology *15*, 21. https://doi.org/10.1186/s12977-018-0404-7.
15. Ho, Y.C., Shan, L., Hosmane, N.N., Wang, J., Laskey, S.B., Rosenbloom, D.I.S., Lai, J., Blankson, J.N., Siliciano, J.D., and Siliciano, R.F. (2013). Replication-competent noninduced proviruses in the latent reservoir increase barrier to HIV-1 cure. Cell *155*, 540–551. https://doi.org/10.1016/j.cell.2013.09.020.
16. Hiener, B., Eden, J.-S., Horsburgh, B.A., and Palmer, S. (2018). Amplification of Near Full-length HIV-1 Proviruses for Next-Generation Sequencing. J. Vis. Exp. *140*, 58016. https://doi.org/10.3791/58016.
17. Wonderlich, E.R., Reece, M.D., and Kulpa, D.A. (2022). Ex Vivo Differentiation of Resting CD4+ T Lymphocytes Enhances Detection of Replication Competent HIV-1 in Viral Outgrowth Assays. Methods Mol. Biol. *2407*, 315–331. https://doi.org/10.1007/978-1-0716-1871-4_21.

18. Busman-Sahay, K., Starke, C.E., Nekorchuk, M.D., and Estes, J.D. (2021). Eliminating HIV reservoirs for a cure: the issue is in the tissue. Curr. Opin. HIV AIDS *16*, 200–208. https://doi.org/10.1097/COH.0000000000000688.

19. Rabezanahary, H., Moukambi, F., Palesch, D., Clain, J., Racine, G., Andreani, G., Benmadid-Laktout, G., Zghidi-Abouzid, O., Soundaramourty, C., Tremblay, C., et al. (2020). Despite early antiretroviral therapy effector memory and follicular helper CD4 T cells are major reservoirs in visceral lymphoid tissues of SIV-infected macaques. Mucosal Immunol. *13*, 149–160. https://doi.org/10.1038/s41385-019-0221-x.

20. Klein, K., Nickel, G., Nankya, I., Kyeyune, F., Demers, K., Ndashimye, E., Kwok, C., Chen, P.-L., Rwambuya, S., Poon, A., et al. (2018). Higher sequence diversity in the vaginal tract than in blood at early HIV-1 infection. PLoS Pathog. *14*, e1006754. https://doi.org/10.1371/journal.ppat.1006754.

21. Donoso, M., D'Amico, D., Valdebenito, S., Hernandez, C.A., Prideaux, B., and Eugenin, E.A. (2022). Identification, Quantification, and Characterization of HIV-1 Reservoirs in the Human Brain. Cells *11*, 2379. https://doi.org/10.3390/cells11152379.

22. Dufour, C., Ruiz, M.J., Pagliuzza, A., Richard, C., Shahid, A., Fromentin, R., Ponte, R., Cattin, A., Wiche Salinas, T.R., Salahuddin, S., et al. (2023). Near full-length HIV sequencing in multiple tissues collected postmortem reveals shared clonal expansions across distinct reservoirs during ART. Cell Rep. *42*, 113053. https://doi.org/10.1016/j.celrep.2023.113053.

23. Mavigner, M., Habib, J., Deleage, C., Rosen, E., Mattingly, C., Bricker, K., Kashuba, A., Amblard, F., Schinazi, R.F., Lawson, B., et al. (2018). Simian Immunodeficiency Virus Persistence in Cellular and Anatomic Reservoirs in Antiretroviral Therapy-Suppressed Infant Rhesus Macaques. J. Virol. *92*, e00562-18. https://doi.org/10.1128/jvi.00562-18.

24. Garcia-Tellez, T., Huot, N., Ploquin, M.J., Rascle, P., Jacquelin, B., and Müller-Trutwin, M. (2016). Non-human primates in HIV research: Achievements, limits and alternatives. Infect. Genet. Evol. *46*, 324–332. https://doi.org/10.1016/j.meegid.2016.07.012.

25. Fisher, B.S., Green, R.R., Brown, R.R., Wood, M.P., Hensley-McBain, T., Fisher, C., Chang, J., Miller, A.D., Bosche, W.J., Lifson, J.D., et al. (2018). Liver macrophage-associated inflammation correlates with SIV burden and is substantially reduced following cART. PLoS Pathog. *14*, e1006871. https://doi.org/10.1371/journal.ppat.1006871.

26. Jambo, K.C., Banda, D.H., Kankwatira, A.M., Sukumar, N., Allain, T.J., Heyderman, R.S., Russell, D.G., and Mwandumba, H.C. (2014). Small alveolar macrophages are infected preferentially by HIV and exhibit impaired phagocytic function. Mucosal Immunol. *7*, 1116–1126. https://doi.org/10.1038/mi.2013.127.

27. Byrnes, S.J., Busman-Sahay, K., Angelovich, T.A., Younger, S., Taylor-Brill, S., Nekorchuk, M., Bondoc, S., Dannay, R., Terry, M., Cochrane, C.R., et al. (2023). Chronic immune activation and gut barrier dysfunction is associated with neuroinflammation in ART-suppressed SIV+ rhesus macaques. PLoS Pathog. *19*, e1011290. https://doi.org/10.1371/journal.ppat.1011290.

28. Estes, J.D., Kityo, C., Ssali, F., Swainson, L., Makamdop, K.N., Del Prete, G.Q., Deeks, S.G., Luciw, P.A., Chipman, J.G., Beilman, G.J., et al. (2017). Defining total-body AIDS-virus burden with implications for curative strategies. Nat. Med. *23*, 1271–1276. https://doi.org/10.1038/nm.4411.

29. Obregon-Perko, V., Bricker, K.M., Mensah, G., Uddin, F., Rotolo, L., Vanover, D., Desai, Y., Santangelo, P.J., Jean, S., Wood, J.S., et al. (2021). Dynamics and origin of rebound viremia in SHIV-infected infant macaques following interruption of long-term ART. JCI Insight *6*, e152526. https://doi.org/10.1172/jci.insight.152526.

30. Solis-Leal, A., Boby, N., Mallick, S., Cheng, Y., Wu, F., De La Torre, G., Dufour, J., Alvarez, X., Shivanna, V., Liu, Y., et al. (2023). Lymphoid tissues contribute to plasma viral clonotypes early after antiretroviral therapy interruption in SIV-infected rhesus macaques. Sci. Transl. Med. *15*, eadi9867. https://doi.org/10.1126/scitranslmed.adi9867.

31. Kearney, M.F., Wiegand, A., Shao, W., Coffin, J.M., Mellors, J.W., Lederman, M., Gandhi, R.T., Keele, B.F., and Li, J.Z. (2016). Origin of Rebound Plasma HIV Includes Cells with Identical Proviruses That Are Transcriptionally Active before Stopping of Antiretroviral Therapy. J. Virol. *90*, 1369–1376. https://doi.org/10.1128/JVI.02139-15.

32. Liu, P.T., Keele, B.F., Abbink, P., Mercado, N.B., Liu, J., Bondzie, E.A., Chandrashekar, A., Borducchi, E.N., Hesselgesser, J., Mish, M., et al. (2020). Origin of rebound virus in chronically SIV-infected Rhesus monkeys following treatment discontinuation. Nat. Commun. *11*, 5412. https://doi.org/10.1038/s41467-020-19254-2.

33. Chun, T.-W., Justement, J.S., Murray, D., Hallahan, C.W., Maenza, J., Collier, A.C., Sheth, P.M., Kaul, R., Ostrowski, M., Moir, S., et al. (2010). Rebound of plasma viremia following cessation of antiretroviral therapy despite profoundly low levels of HIV reservoir: implications for eradication. AIDS *24*, 2803–2808. https://doi.org/10.1097/QAD.0b013e328340a239.

34. Le, T., Farrar, J., and Shikuma, C. (2011). Rebound of plasma viremia following cessation of antiretroviral therapy despite profoundly low levels of HIV reservoir: implications for eradication. AIDS *25*, 871–873. https://doi.org/10.1097/QAD.0b013e32834490b1.

35. Long, S., Fennessey, C.M., Newman, L., Reid, C., O'Brien, S.P., Li, Y., Del Prete, G.Q., Lifson, J.D., Gorelick, R.J., and Keele, B.F. (2019). Evaluating the Intactness of Persistent Viral Genomes in Simian Immunodeficiency Virus-Infected Rhesus Macaques after Initiating Antiretroviral Therapy within One Year of Infection. J. Virol. *94*, e01308-19. https://doi.org/10.1128/JVI.01308-19.

36. Bender, A.M., Simonetti, F.R., Kumar, M.R., Fray, E.J., Bruner, K.M., Timmons, A.E., Tai, K.Y., Jenike, K.M., Antar, A.A.R., Liu, P.T., et al. (2019). The Landscape of Persistent Viral Genomes in ART-Treated SIV, SHIV, and HIV-2 Infections. Cell Host Microbe *26*, 73–85. https://doi.org/10.1016/j.chom.2019.06.005.

37. Kumar, M.R., Fray, E.J., Bender, A.M., Zitzmann, C., Ribeiro, R.M., Perelson, A.S., Barouch, D.H., Siliciano, J.D., and Siliciano, R.F. (2023). Biphasic decay of intact SHIV genomes following initiation of antiretroviral therapy complicates analysis of interventions targeting the reservoir. Proc. Natl. Acad. Sci. USA *120*, e2313209120. https://doi.org/10.1073/pnas.2313209120.

38. Fray, E.J., Wu, F., Simonetti, F.R., Zitzmann, C., Sambaturu, N., Molina-Paris, C., Bender, A.M., Liu, P.-T., Ventura, J.D., Wiseman, R.W., et al. (2023). Antiretroviral therapy reveals triphasic decay of intact SIV genomes and persistence of ancestral variants. Cell Host Microbe *31*, 356–372. https://doi.org/10.1016/j.chom.2023.01.016.

39. Banga, R., Procopio, F.A., Lana, E., Gladkov, G.T., Roseto, I., Parsons, E.M., Lian, X., Armani-Tourret, M., Bellefroid, M., Gao, C., et al. (2023). Lymph node dendritic cells harbor inducible replication-competent HIV despite years of suppressive ART. Cell Host Microbe *31*, 1714–1731. https://doi.org/10.1016/j.chom.2023.08.020.

40. Oliva, H., Pacheco, R., Martinez-Navio, J.M., Rodríguez-García, M., Naranjo-Gómez, M., Climent, N., Prado, C., Gil, C., Plana, M., García, F., et al. (2016). Increased expression with differential subcellular location of cytidine deaminase APOBEC3G in human CD4 $^{+}$ T-cell activation and dendritic cell maturation. Immunol. Cell Biol. *94*, 689–700. https://doi.org/10.1038/icb.2016.28.

41. Gantner, P., Pagliuzza, A., Pardons, M., Ramgopal, M., Routy, J.P., Fromentin, R., and Chomont, N. (2020). Single-cell TCR sequencing reveals phenotypically diverse clonally expanded cells harboring inducible HIV proviruses during ART. Nat. Commun. *11*, 4089. https://doi.org/10.1038/s41467-020-17898-8.

42. Maldarelli, F., Wu, X., Su, L., Simonetti, F.R., Shao, W., Hill, S., Spindler, J., Ferris, A.L., Mellors, J.W., Kearney, M.F., et al. (2014). Specific HIV integration sites are linked to clonal expansion and persistence of infected cells. Science *345*, 179–183. https://doi.org/10.1126/science.1254194.

43. Simonetti, F.R., Sobolewski, M.D., Fyne, E., Shao, W., Spindler, J., Hattori, J., Anderson, E.M., Watters, S.A., Hill, S., Wu, X., et al. (2016). Clonally expanded CD4+ T cells can produce infectious HIV-1 in vivo. Proc. Natl. Acad. Sci. USA *113*, 1883–1888. https://doi.org/10.1073/pnas.1522675113.

44. Wagner, T.A., McLaughlin, S., Garg, K., Cheung, C.Y.K., Larsen, B.B., Styrchak, S., Huang, H.C., Edlefsen, P.T., Mullins, J.I., and Frenkel, L.M. (2014). Proliferation of cells with HIV integrated into cancer genes contributes to persistent infection. Science *345*, 570–573. https://doi.org/10.1126/science.1256304.

45. Cohn, L.B., Silva, I.T., Oliveira, T.Y., Rosales, R.A., Parrish, E.H., Learn, G.H., Hahn, B.H., Czartoski, J.L., McElrath, M.J., Lehmann, C., et al. (2015). HIV-1 Integration Landscape during Latent and Active Infection. Cell *160*, 420–432. https://doi.org/10.1016/j.cell.2015.01.020.

46. Hosmane, N.N., Kwon, K.J., Bruner, K.M., Capoferri, A.A., Beg, S., Rosenbloom, D.I.S., Keele, B.F., Ho, Y.C., Siliciano, J.D., and Siliciano, R.F. (2017). Proliferation of latently infected CD4+ T cells carrying replication-competent HIV-1: Potential role in latent reservoir dynamics. J. Exp. Med. *214*, 959–972. https://doi.org/10.1084/jem.20170193.

47. Ferris, A.L., Wells, D.W., Guo, S., Del Prete, G.Q., Swanstrom, A.E., Coffin, J.M., Wu, X., Lifson, J.D., and Hughes, S.H. (2019). Clonal expansion of SIV-infected cells in macaques on antiretroviral therapy is similar to that of HIV-infected cells in humans. PLoS Pathog. *15*, e1007869. https://doi.org/10.1371/journal.ppat.1007869.

48. Perreau, M., Savoye, A.-L., De Crignis, E., Corpataux, J.-M., Cubas, R., Haddad, E.K., De Leval, L., Graziosi, C., and Pantaleo, G. (2013). Follicular helper T cells serve as the major CD4 T cell compartment for HIV-1 infection, replication, and production. J. Exp. Med. *210*, 143–156. https://doi.org/10.1084/jem.20121932.

49. Deleage, C., Wietgrefe, S.W., Del Prete, G., Morcock, D.R., Hao, X.-P., Piatak, M., Jr., Bess, J., Anderson, J.L., Perkey, K.E., Reilly, C., et al. (2016). Defining HIV and SIV Reservoirs in Lymphoid Tissues. Pathog. Immun. *1*, 68–106. https://doi.org/10.20411/pai.v1i1.100.

50. Bronnimann, M.P., Skinner, P.J., and Connick, E. (2018). The B-cell follicle in HIV infection: Barrier to a cure. Front. Immunol. *9*, 20. https://doi.org/10.3389/fimmu.2018.00020.

51. Heesters, B.A., Lindqvist, M., Vagefi, P.A., Scully, E.P., Schildberg, F.A., Altfeld, M., Walker, B.D., Kaufmann, D.E., and Carroll, M.C. (2015). Follicular Dendritic Cells Retain Infectious HIV in Cycling Endosomes. PLoS Pathog. *11*, e1005285. https://doi.org/10.1371/journal.ppat.1005285.

52. Garber, J.C., Barbee, R.W., Bielitzki, J.T., Clayton, L.A., Donovan, J.C., Hendricksen, C.F.M., Kohn, D.F., Lipman, N.S., Locke, P.A., Melcher, J., et al. (2011). GUIDE FOR THE CARE AND USE OF LABORATORY ANIMALS, 8th edition (The National Academies Press).

53. Nishimura, Y., Shingai, M., Willey, R., Sadjadpour, R., Lee, W.R., Brown, C.R., Brenchley, J.M., Buckler-White, A., Petros, R., Eckhaus, M., et al. (2010). Generation of the Pathogenic R5-Tropic Simian/Human Immunodeficiency Virus SHIV $_{AD8}$ by Serial Passaging in Rhesus Macaques. J. Virol. *84*, 4769–4781. https://doi.org/10.1128/JVI.02279-09.

54. Del Prete, G.Q., Smedley, J., Macallister, R., Jones, G.S., Li, B., Hattersley, J., Zheng, J., Piatak, M., Keele, B.F., Hesselgesser, J., et al. (2016). Short Communication: Comparative Evaluation of Coformulated Injectable Combination Antiretroviral Therapy Regimens in Simian Immunodeficiency Virus-Infected Rhesus Macaques. AIDS Res. Hum. Retrovir. *32*, 163–168. https://doi.org/10.1089/aid.2015.0130.

55. Micci, L., Ryan, E.S., Fromentin, R., Bosinger, S.E., Harper, J.L., He, T., Paganini, S., Easley, K.A., Chahroudi, A., Benne, C., et al. (2015). Interleukin-21 combined with ART reduces inflammation and viral reservoir in SIV-infected macaques. J. Clin. Investig. *125*, 4497–4513. https://doi.org/10.1172/JCI81400.

56. Ryan, E.S., Micci, L., Fromentin, R., Paganini, S., McGary, C.S., Easley, K., Chomont, N., and Paiardini, M. (2016). Loss of Function of Intestinal IL-17 and IL-22 Producing Cells Contributes to Inflammation and Viral Persistence in SIV-Infected Rhesus Macaques. PLoS Pathog. *12*, e1005412. https://doi.org/10.1371/journal.ppat.1005412.

57. Li, H., Wang, S., Kong, R., Ding, W., Lee, F.-H., Parker, Z., Kim, E., Learn, G.H., Hahn, P., Policicchio, B., et al. (2016). Envelope residue 375 substitutions in simian–human immunodeficiency viruses enhance CD4 binding and replication in rhesus macaques. Proc. Natl. Acad. Sci. USA *113*, E3413–E3422. https://doi.org/10.1073/pnas.1606636113.

58. O'Brien, S.P., Swanstrom, A.E., Pegu, A., Ko, S.-Y., Immonen, T.T., Del Prete, G.Q., Fennessey, C.M., Gorman, J., Foulds, K.E., Schmidt, S.D., et al. (2019). Rational design and in vivo selection of SHIVs encoding transmitted/founder subtype C HIV-1 envelopes. PLoS Pathog. *15*, e1007632. https://doi.org/10.1371/journal.ppat.1007632.

59. Keele, B.F., Giorgi, E.E., Salazar-Gonzalez, J.F., Decker, J.M., Pham, K.T., Salazar, M.G., Sun, C., Grayson, T., Wang, S., Li, H., et al. (2008). Identification and characterization of transmitted and early founder virus envelopes in primary HIV-1 infection. Proc. Natl. Acad. Sci. USA *105*, 7552–7557. https://doi.org/10.1073/pnas.0802203105.

STAR★METHODS

KEY RESOURCES TABLE

REAGENT or RESOURCE	SOURCE	IDENTIFIER
Bacterial and virus strains		
SHIV-AD8-EO	Dr. Malcolm Martin	NCBITaxon_57667
Biological samples		
Rhesus macaques derived blood, lymph nodes biopsies (inguinal or axillary) and colon biopsies	Wisconsin National Primate Research Center (WNPRC)	N/A
Deposited data		
SHIV full-length genomic sequences	GenBank	BankIt2921480: PV068831 - PV068975
SHIV *env* sequences	GenBank	BankIt2875156: PQ380606-PQ380700
Experimental models: Organisms/strains		
Rhesus macaques (Macaca mulatta) of Indian ancestry	Wisconsin National Primate Research Center (WNPRC)	NCBITaxon_9544
Oligonucleotides		
SIV U3 Fw1: 5′-CAG AAG AGT TTG GAA GCA AGT C-3′	Integrated DNA technologies	N/A
SIV U3 Rv1: 5′-ACA TAT GCC TCA TAA GTG TAG G-3′	Integrated DNA technologies	N/A
SIV U3 Fw2: 5′-TTA GAA GAA GGC TAA CCG CAA G-3′	Integrated DNA technologies	N/A
SIV U3 Rv2: 5′-TTG GAT CAA ACT TCC ATG CTA G-3′	Integrated DNA technologies	N/A
SHIV env reverse primer: 5′-TGT AAT AAA TCC CTT CCA GTC CCC CC-3′	Integrated DNA technologies	N/A
SIVLLTR Fw: 5' – ATG CCA CGT AAG CGA AAC TGG CAG ATT GAG CCC TGG GAG – 3′	Integrated DNA technologies	N/A
SIVgag Rev: 5' – TGC TGC CCA TAC TAC ATG CTT C – 3′	Integrated DNA technologies	N/A
LambdaT: 5' – ATG CCA CGT AAG CGA AAC T – 3′	Integrated DNA technologies	N/A
SIVLTR Rev2: 5' – CTT TAA GCA AGC AAG CGT GGA G – 3′	Integrated DNA technologies	N/A
5' –/56-FAM/GCA GGTAGA/ZEN/GCC TGG GTG TTC CCTGC/3IABkFQ/– 3′	Integrated DNA technologies	N/A
HCD3 out 5': 5' – ACT GAC ATG GAA CAG GGG AAG – 3′	Integrated DNA technologies	N/A
HCD3 out 3': 5' – CCA GCT CTG AAG TAG GGA ACA TAT – 3′	Integrated DNA technologies	N/A
HCD3 in 5': 5′-GGC TAT CAT TCT TCT TCA AGG T-3′	Integrated DNA technologies	N/A
Mamu CD3 in 3': 5' – TAA GAT GGC GGT AAC AGG GT – 3′	Integrated DNA technologies	N/A
MamuCD3Zen 5' –/56-FAM/AGC AGA GAA/ZEN/CAG TTA AGA GGC TCC AT/3IABkFQ/– 3′	Integrated DNA technologies	N/A
Software and algorithms		
Lima PacBio software v2.7.1	DNA Link, South Korea	SCR_025520
pbAA PacBio algorithm v1.0.3	DNA Link, South Korea	SCR_017988
Multiple Fast Fourier transform algorithm	Los Alamos National Laboratory	SCR_011811
Geneious Prime (v2021.1.1)	https://www.geneious.com/	SCR_010519
HIV Database QC Tool	Los Alamos National Laboratory	SCR_002906
HIV Database Gene Cutter online tool	Los Alamos National Laboratory	SCR_002906
HIV Database Elim Dupes online tool	Los Alamos National Laboratory	SCR_002906
GraphPad Prism v9.3.0	https://www.graphpad.com/	SCR_002798
IQ-TREE	http://www.iqtree.org/	SCR_017254

EXPERIMENTAL MODEL AND STUDY PARTICIPANT DETAILS

A total of 5 Rhesus macaques (Macaca mulatta) 2 females and 3 males, of Indian ancestry and free of simian retrovirus type D (SRV), simian T-lymphotropic virus type 1 (STLV-1), SIV and macacine herpesvirus 1 (herpesvirus B) were used for these studies (Table S1).

These animals housed at the Wisconsin National Primate Research Center (WNPRC) in accordance with the standards of the Association for the Assessment and Accreditation of Laboratory Animal Care (AAALAC) and the University of Wisconsin Research Animal Resources Center and Compliance unit (UWRARC). Animal experiments were approved by the University of Wisconsin College of Letters and Sciences and the Vice Chancellor for Research and Graduate Education Centers AICUC (protocol numbers G005609 and G006679) and performed in compliance with the principles described in the *Guide for the Care and Use of Laboratory Animals*.[52] Fresh water was always available, commercial monkey chow was provided twice a day and fresh produce was supplied daily. To minimize any pain and distress related to experimental procedures, Ketamine HCL was used to sedate animals prior to blood collection and animals were monitored twice a day by animal care and veterinary staff. The animals were socially housed in pairs or groups of compatible animals whenever possible. Animals were infected intravenously with the viral strain SHIV-AD8-EO (200 TCID50).[53] Animals were started on ART at week 8 post-infection and remained on therapy for 29 weeks until week 37. A solution of the antiretroviral drugs dolutegravir (DTG, 2.5 mg/mL), tenofovir disoproxil fumarate (TDF, 5.1 mg/mL) and emtricitabine (FTC, 40 mg/mL) was prepared in 15% Kleptose (HPB Biopharma, cat. 346113105E), filter-sterilized through a 0.2 μm nylon membrane and stored at −20°C. Each animal received daily subcutaneous injections of ART at doses of 1 mL per kg body weight.[54]

Animals age was in average 8.4 years (4.2–12.8) at the moment of sampling. Blood, lymph nodes biopsies (inguinal or axillary) and colon biopsies were obtained from all animals at weeks 34, 36, 38 and 40. The gut biopsies were pinch biopsies taken from the colon. All the tissue recovered was used for DNA/RNA dual extraction following the protocol described below. Lymph node biopsies were obtained with forceps using sharp or blunt dissection, collecting one lymph node if large (∼1 cm diameter) or multiple small lymph nodes. Biopsies were homogenized and passed through a 70-μm cell strainer to mechanically isolate lymphocytes. From blood samples, mononuclear cells were isolated by density gradient centrifugation. Plasma samples were obtained at week 40 (Figure 1A).

METHOD DETAILS

DNA and RNA extractions

CD4 T cell were enriched from blood and lymph nodes mononuclear cells using the EasySep Human $CD4^+$ T cell Isolation Kit (StemCell). Colon biopsies were thawed, lysed and homogenized in RLTPlus lysis buffer (Qiagen) at room temperature using the RNA program of the gentleMACS Dissociator (Miltenyi). DNA and RNA were simultaneously extracted using the AllPrep DNA/RNA/miRNA Universal Kit (Qiagen), according to the manufacturer's instructions.

SHIV DNA and RNA quantifications

Total SHIV DNA and cell-associated SHIV RNA were measured by ultrasensitive nested qPCR with primers annealing the LTR/gag region. SIVLLTR Fw: 5' – ATG CCA CGT AAG CGA AAC TGG CAG ATT GAG CCC TGG GAG – 3'; SIVgag Rev: 5' – TGC TGC CCA TAC TAC ATG CTT C – 3'; LambdaT: 5' – ATG CCA CGT AAG CGA AAC T – 3'; SIVLTR Rev2: 5' – CTT TAA GCA AGC AAG CGT GGA G – 3'; 5' –/56-FAM/GCA GGTAGA/ZEN/GCC TGG GTG TTC CCTGC/3IABkFQ/– 3'.[55,56] Primers specific for the CD3 gene were added to the DNA PCR reaction to precisely quantify the cell input: HCD3 out 5': 5' – ACT GAC ATG GAA CAG GGG AAG – 3'; HCD3 out 3': 5' – CCA GCT CTG AAG TAG GGA ACA TAT – 3'; HCD3 in 5': 5′-GGC TAT CAT TCT TCT TCA AGG T-3'; Mamu CD3 in 3': 5' – TAA GAT GGC GGT AAC AGG GT – 3'; MamuCD3Zen 5' –/56-FAM/AGC AGA GAA/ZEN/CAG TTA AGA GGC TCC AT/3IABkFQ/– 3'. The first-round PCR cycle conditions were as follows: a denaturation step of 8 min at 95°C and 12 cycles of amplification (95°C for 1 min, 55°C for 40 s, 72°C for 1 min), followed by a final elongation step at 72°C for 15 min. For the cell-associated RNA a 30 min incubation at 50°C was included previous to the previous cycling protocol. The second rounds of PCR were carried out in real time as follows: denaturation step (95°C for 4 min), followed by 40 cycles of amplification (95°C for 3 s, 60°C for 10 s).

The number of copies of total SHIV DNA were calculated by using serial dilutions of lysed 3D8 cells as a standard curve. The amount of total cell-associated SHIV RNA was calculated by using serial dilutions of *in vitro* transcribe SHIV RNA as standard. All measures were performed in triplicate wells. Results were expressed as numbers of SHIV genomes or transcripts per million cells.

Near full-length amplification of SHIV genomes

Near full-length amplification of proviral sequences was performed at an endpoint dilution of the extracted DNA where <30% of the reactions were positive, obtaining a total of 144 SHIV proviral sequences. The protocol was adapted from previous studies.[11,22] Briefly, the first-round PCR cycle conditions were as follows: a denaturation step of 30 s at 98°C and 25 cycles of amplification (98°C for 10 s, 60°C for 10 s, 72°C for 5 min), followed by a final elongation step at 72°C for 5 min.

SHIV proviruses were pre-amplified using an Invitrogen Platinum SuperFi II MasterMix (ThermoFisher cat.12358050) with two outer primers (SIV U3 Fw1: 5′-CAG AAG AGT TTG GAA GCA AGT C-3'; SIV U3 Rv1: 5′-ACA TAT GCC TCA TAA GTG TAG G-3′). Diluted pre-amplification products were used in a second round of amplification, using inner primers (SIV U3 Fw2: 5′-TTA GAA GAA GGC TAA CCG CAA G-3'; SIV U3 Rv2: 5′-TTG GAT CAA ACT TCC ATG CTA G-3′). The second round of PCR was carried out as follows: denaturation step of 30 s at 98°C and 30 cycles of amplification (98°C for 10 s, 60°C for 10 s, 72°C for 5 min), followed by a final elongation step at 72°C for 5 min.

3D8 extracted DNA were used as positive controls for PCR amplification. Proviral amplification was confirmed by running a fraction of the PCR products on an 0.8% agarose gel. Wells containing an amplicon of approximately 700 bp, indicative of the amplification of

a 2-LTR junction, were discarded. PCR reactions with two bands of different sizes were not excluded, since the sequencing method can discriminate between two sequences present in the same reaction.

PacBio sequencing

All amplicons were sequenced using the PacBio next-generation sequencing platform. Each SHIV pre-amplified DNA were re-amplified with barcoded inner PCR primers (96 different PacBio barcodes). Barcoded amplicons were purified using AMPure XP beads (Beckman Coulter), following the manufacturer's instructions, prior to Nanodrop quantification. 50 ng of each of the 96-barcoded amplicons were pooled together and sequenced on a Sequel or Sequel II instrument (DNA Link, South Korea).

PacBio demultiplexing and cleaning

The demultiplex barcodes analysis was powered by the Lima PacBio software v2.7.1. High-quality phased consensus sequences representing near full-length SHIV genome sequences with high fidelity and without the need for reconstruction were generated with the pbAA PacBio algorithm v1.0.3. Any sequences that did not blast with the SHIV-AD8-EO reference sequence stored in the GenBank (MN816822.1), or that lacked one of the primer's sequences, were discarded from further analysis.

Integrity analysis

Sequences containing only LTR portions of the viral genome, which likely corresponded to 2-LTR circles amplifications, were excluded from the analysis. All proviral sequences were aligned to the reference SHIV-AD8-EO sequence using Multiple Fast Fourier transform program (MAFFT) with strategy E-INS-i and a scoring matrix of 1PAM/k = 2 (online https://mafft.cbrc.jp/alignment/server/ or with Geneious Prime (v2021.1.1) pluggin). For integrity analysis, all sequences containing (in this order) hypermutations, large internal deletions, stop codons and/or frameshift, defects in the Ψ locus, small internal deletions in a coding region, inversions or insertions were considered defective. Inversions and insertions were detected manually in the alignment. Hypermutations were detected using the online HIV Database QC Tool (https://www.hiv.lanl.gov/content/sequence/QC/index.html). Genomes with large internal deletions were defined as any provirus shorter than 8,500 bp (excluding the primer's regions). Stop codons/frameshifts were identified using the HIV Database Gene Cutter online tool (www.hiv.lanl.gov/content/sequence/GENE_CUTTER/cutter). Any defect in the Ψ locus (MSD point mutation; stem loop 2 deletion; packaging signal deletion) were determined manually by looking at the alignment with the reference SHIV-AD8-EO sequence. The intactness of the 9 coding regions (gag, pol, vif, vpx, tat, rev, vpu, nef, env) and 2 regulatory regions (Ψ and RRE) were evaluated by assessing the presence of a start codon (except for pol), and the lack of internal stop codons, frameshift or small deletion over 3% of the ORF's length.

Clonality analysis

Clonal sequences were defined as proviral amplicons 100% identical to each other and were determined using the HIV Database Elim Dupes online tool (https://www.hiv.lanl.gov/content/sequence/elimdupesv2/elimdupes.html) and confirmed using the Geneious Prime diversity tool. Phylogenetic trees were built with IQ-Tree2, using a Maximum-likelihood tree GTR + I + G model, 1,000 bootstraps.

Env sequencing

Virion-derived Env sequences were obtained from plasma samples by single copy sequencing. Viral RNA was isolated from plasma-associated virions as described previously.[57] RNA was reverse transcribed into cDNA which was then used for subsequent dilution and single genome PCR amplification and SHIV Env sequencing as described previously.[58] Briefly, cDNA was generated from viral RNA using the SHIV specific primer 5′-TGT AAT AAA TCC CTT CCA GTC CCC CC-3′ and SuperScript III reverse transcriptase as per the manufacturer's instructions (ThermoFisher Scientific). Template viral cDNA was diluted until the number of wells containing a viral template constituted 30% or less of the total number of PCR wells to ensure a single viral genome per reaction, as calculated by Poisson distribution statistics.[59] The SHIV envelope gene was amplified using a two-round nested PCR with SHIV specific primers and Platinum Taq DNA High Fidelity polymerase (ThermoFisher Scientific) per the manufacturer's instructions. Correctly sized amplicons identified by gel electrophoresis were sequenced by Sanger sequencing using BigDye Terminator technology (Applied Biosystems) and gene specific primers. Overlapping sequence fragments were assembled into contigs using Sequencher (Gene Codes), and chromatograms were manually checked for multiple peaks to confirm single genome sequencing. Sequences with mixed bases were excluded from further analysis. *env* RNA sequences were compared to proviral Env sequences obtained from tissues obtained prior to ATI using the HIV Database Elim Dupes as described above. Intact proviral- and virion-derived *env* sequences were used to build phylogenetic trees with the algorith IQ-Tree2, using a Maximum-likelihood tree GTR + I + G model, 1,000 bootstraps. From these phylogenetic trees, the total branch length between each plasma viral particle sequence and the closest intact proviral sequence was obtained.

QUANTIFICATION AND STATISTICAL ANALYSIS

All data were analyzed using GraphPad Prism v9.3.0. Statistical tests are indicated in the figure legends. A p value of less than 0.05 was considered statistically significant.